

# Improvisation of Structural, Electrical and Magnetic Properties of Nanocrystalline $\text{Ca}_2\text{-Y}$ Hexaferrite on Al-Substitution

P. R. Moharkar<sup>a\*</sup>, S. R. Gawali<sup>b</sup>, K. G. Rewatkar<sup>c</sup>, V. M. Nanoti<sup>d</sup>

<sup>a\*</sup>Department of Physics, A. C. S. College, Chandrapur, (M.S), India (442401)

<sup>b</sup>Department Physics, Dr. Ambedkar College, Chandrapur, (M.S), India (442401)

<sup>c</sup>Department of Physics, Dr. Ambedkar College, Nagpur, (M.S), India (440010)

<sup>d</sup>Priyadarshini College of Engineering, Nagpur, Maharashtra State, India (440019)

\*Corresponding author.

## ABSTRACT

Calcium hexaferrites doped with  $\text{Al}^{3+}$  ion,  $\text{Ca}_2\text{Zn}_2\text{Fe}_{12-x}\text{Al}_x\text{O}_{22}$  ( $x=0, 0.7$  and  $1.0$ ) were prepared microwave induced sol-gel combustion technique. The structure properties of the calcined samples were studied using powder X-ray diffraction (XRD). All the XRD patterns showed the single phase of the Y-type calcium hexaferrites without other intermediate phase. The lattice parameters of the synthesized sample were found to increase with increase substitution of  $\text{Al}^{3+}$  ion for  $\text{Fe}^{3+}$  ion, which is attributed to the ionic size differences of cations involved. The morphological properties of the synthesized samples were measured by using SEM. The SEM study have shown that the sample exhibit relatively well defined, hexagonal like grains with average size of less than 80 nm. X-ray density was found to decrease with the substitution. The bulk density of the sample was increased whereas the porosity was decreased with the increase in the substitution. The dc electrical conductivity measurements have been carried out over the temperature range 300 K – 800 K by using impedance analyzer. The electrical conductivity of the sample was explained on the basis of hopping mechanism. The resistivity of the sample was found to be enhanced with the substitution of  $\text{Al}^{3+}$  ion for  $\text{Fe}^{3+}$  ion which has potential applications in microwave devices. The magnetic properties of the sample at room temperature were studied by VSM. The coercivity of the sample was found to be enhanced which enable its use as a permanent magnet.

**Keywords:** Y-type hexagonal ferrite, Nanoparticles, Electrical and Magnetic properties etc.

## 1. INTRODUCTION

Y-type ferrite  $\text{Ba}_2\text{Zn}_2\text{Fe}_{12}\text{O}_{22}$  was first studied by Jonkar [1] in the year 1956 and after that Kojima [2] in 1982 was discovered that the ferrites were hexagonal in structure. The interest of researchers in the field of hexagonal ferrites is increasing due to their use as permanent magnet [3], microwave device materials and magneto-optic recording media [4]. It is possible to synthesize a ferrite of specific properties, by controlling the chemical composition and nature of substituting element [5]. The widely studied Y-type hexagonal ferrites is  $\text{Ba}_2\text{Zn}_2\text{Fe}_{12}\text{O}_{22}$ . The Y-type hexagonal ferrites have a crystalline structure built up as a superposition of S and T blocks. The unit cell is composed of the sequence STSTST including three formula units. The metallic cations are distributed among six sublattices as two tetrahedral and

four octahedral sublattices. It is worth noting that inside the T block, three octahedral ions, belonging to  $6c_{VI}$  and  $3b_{VI}$  sublattices, lies on a vertical threefold axis, the central  $3b_{VI}$  ion sharing two faces of its coordination figure with the adjacent  $6c_{VI}$  ions. Such a configuration, as already pointed out, is responsible for a higher potential energy of the structure due to a stronger electrostatic repulsion between the cations; therefore such sites are likely to be preferred by low charge ions. As a consequence a non-magnetic  $\text{Me}^{2+}$  ions with a marked preference for the octahedral coordination may cause drastic changes in the magnetic configuration with respect to the usual Gorter scheme; indeed the occupation of either  $6c_{VI}$  or  $3b_{VI}$  by non-magnetic ions leads to the cancellation of the antiferromagnetic  $b_{VI}-c_{IV}^*$  interaction which is the strongest one in the Y-structure. The substitution of  $\text{Ba}^{2+}$  ion by other divalent cations (i.e.  $\text{Ca}^{2+}$  ions in present case) does not affect the site distribution [6].

The present module of research aims to synthesize Y-type substituted calcium hexaferrites by microwave induced sol-gel combustion method which facilitates the production of ultra fine hexagonal ferrite particles especially in nanoscale and to study the effect of composition on structural, electrical and magnetic properties of it.

## 2. EXPERIMENTAL

### 2.1. Sample preparations

The series of  $\text{Al}^{3+}$  ion substituted hexaferrite samples with formula  $\text{Ca}_2\text{Zn}_2\text{Fe}_{12-x}\text{Al}_x\text{O}_{22}$  ( $x=0; 0.7$  and  $1$ ) were synthesized by microwave induced sol-gel combustion technique. The starting materials to synthesized nanostructured hexaferrite samples are AR grade  $\text{Ca}(\text{NO}_3)_2 \cdot 4\text{H}_2\text{O}$ ,  $\text{Fe}(\text{NO}_3)_3 \cdot 9\text{H}_2\text{O}$ ,  $\text{Zn}(\text{NO}_3)_2 \cdot 4\text{H}_2\text{O}$ ,  $\text{CO}(\text{NH}_2)_2$  and  $\text{Al}(\text{NO}_3)_3 \cdot 9\text{H}_2\text{O}$ . The stoichiometric amounts of AR grade metal nitrates were dissolved in triple filtered deionised distilled water at the temperature of  $50^\circ\text{C}$  in a beaker. These metal nitrates were used as oxidants. The fuel urea  $\text{CO}(\text{NH}_2)_2$  was also dissolve in deionised water and was used as reducing agent to supply requisite energy to initiate exothermic reaction amongst oxidants. This solution of metal nitrates and fuel was put into the microwave oven of 2.45 GHz and is then heated in the digitally controlled microwave oven for 15–20 min. so that it get converted into brown gel. The gel get burnt by self propagating combustion reaction evolving large volumes of gases and finally get converted in homogeneous nanocrystalline brown powder sample. The brown powder samples were crushed in the agate mortar to have fine calcium

hexaferrites powder. The 10% polyvinyl alcohol solution (2–3 drops) had been mixed before they were pressed by hydraulic press into pellets of 15 mm in diameter and about 5–8 mm in thickness using a stainless steel die set under uniaxial appropriate pressure for 5 min. The Poly Vinyl Acetate was used as a binder. The pellets of the sample was calcined at 800 °C for about 2 hours in the electric furnace to obtain monophasic Y-type calcium hexaferrites.

## 2.2 Characterization

The crystalline phase determination of the samples were carried out on Philips Holand XRD unit (PW 1710) operating at 42.5 kV and 18.00mA with Copper K $\alpha$ -radiation with wavelength 1.54056Å. The X-ray diffraction was measured in the range from 20° to 70° with a step of 0.02° for 1 second. XRD pattern was subjected to Debye Scherrer technique to determine the particle size. The morphological properties of the synthesized samples are recorded by using SEM studies using Scanning Electron Microscope (Model JSM- 7600F) having resolution of 1.0nm (15kV), 1.5nm (1kV) accelerating voltage 0.1 to 30 kV, magnification X 25 to 1000000. The electrical conductivity of aluminium substituted calcium ferrite has been measured from 300 to 800K by using impedance analyzer. The magnetization measurement of the synthesized samples were carried out using a vibrating sample magnetometer (VSM) at room temperature with an applied magnetic field of 10kG to achieve saturation state.

## 3. RESULTS AND DISCUSSION

### 3.1. XRD analysis

The XRD pattern are shown in Fig. 1. These patterns are matched with the standard pattern which are best fitted with and no extra lines were detected, which confirm the magnetoplumbite phase as reported in the samples. The space group for the samples was observed to be R $\bar{3}$ m (SG no. 166).

The parameter such as lattice constant (a and c), cell volume (V), X-ray density ( $\rho_{x-ray}$ ), bulk density ( $\rho_m$ ) and porosity are calculated using XRD data, after analysis above mentioned parameters were enumerated in Table 1.

The diffraction pattern of samples also shows the variation in relative intensities, may be attributed to the occupation of various lattice sites by substituted ions. The lattice parameter 'a' and 'c' show decreasing trend with increase in concentration of Al<sup>3+</sup> ions. This variation in relatively small but can be considered due to smaller ionic radii of Al<sup>3+</sup> ions (0.53Å) compared to that Fe<sup>3+</sup> ions (0.64Å) for six fold co-ordination. As a result, the cell volume of Ca<sub>2</sub>-Y ferrites found to have contraction after being doped with Al<sup>3+</sup> ions. This is in agreement with the fact that all the hexagonal types exhibit variation in lattice constant after being substituted by variable size ions as reported by Haneda and Kojima [7], Ounnunkad and Winotai [8]. The X-ray density of the sample is greater than the bulk density. The values of X-ray density decreases while bulk density increases with increase in the concentration of Al<sup>3+</sup> ion in Ca<sub>2</sub>-Y ferrite. The porosity of the sample decreases with increase in the concentration of Al<sup>3+</sup> ion in Ca<sub>2</sub>-Y ferrite.

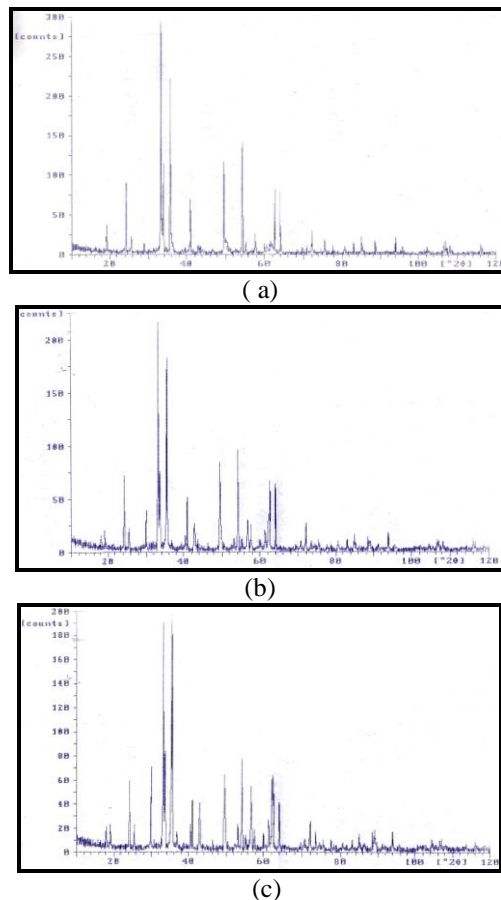


Fig. 1. : X-ray diffraction spectra of Ca<sub>2</sub>Zn<sub>2</sub>Fe<sub>12-x</sub>Al<sub>x</sub>O<sub>22</sub> : (a) x=0, (b)x=0.7 and (c) x=1

**Table 1: Structural Study of  $\text{Ca}_2\text{Zn}_2\text{Fe}_{12-x}\text{Al}_x\text{O}_{22}$  Samples**

| Sample   | X   | a<br>(Å)   | c<br>(Å)    | V<br>(Å) <sup>3</sup> | $\rho_{\text{x-ray}}$<br>(gm/cm <sup>3</sup> ) | $\rho_{\text{m}}$<br>(gm/cm <sup>3</sup> ) | Porosity<br>(%) |
|--|-----|------------|-------------|-----------------------|--|--|-----------------|
| ( $\text{Ca}_2\text{Zn}_2\text{Fe}_{12}\text{O}_{22}$ )                  | 0.0 | 5.039<br>0 | 44.107<br>2 | 1239.2<br>7           | 4.2239   | 3.0982                                     | 26.67           |
| ( $\text{Ca}_2\text{Zn}_2\text{Fe}_{11.3}\text{Al}_{0.7}\text{O}_{22}$ ) | 0.7 | 5.047<br>2 | 44.277<br>6 | 1248.1<br>2           | 4.1257   | 2.9238                                     | 29.14           |
| ( $\text{Ca}_2\text{Zn}_2\text{Fe}_{11}\text{AlO}_{22}$ )                | 1.0 | 5.044<br>6 | 44.205<br>6 | 1244.8<br>9           | 4.1067   | 3.1255                                     | 23.90           |

### 3.2 SEM analysis

Fig 2 shows the SEM micrograph of the samples. The SEM photograph, it can be confirmed that samples exhibit relatively well defined, hexagonal like grains with average size of less than 80nm, as reported by Thompson [9].

### 3.3. DC conductivity

Fig. 3 shows the graphs of electrical conductivity  $\ln(\sigma)$  versus temperature  $\left(\frac{10^3}{T}\right)$  for all the ferrite samples. It has been observed from the graphs that the value of  $\ln(\sigma)$  declines almost linearly with increasing of reciprocal temperature up to a certain temperature known as transition temperature

( $T_i$ ). where there is a change in slope (kink) occurs in plots. The temperature where kink is observed for the various composition of  $\text{Al}^{+3}$  ions in  $\text{Ca}_2\text{-Y}$  ferrites is in neighborhood of magnetic transition temperature (Curie temperature  $T_c$ ). The Curie temperature ( $T_c$ ) of the Al substituted  $\text{Ca}_2\text{-Y}$  hexaferrites have been determined from the susceptibility measurement versus temperature plots as reported in Table 2. This reveals that the kink observed in the aluminium substituted  $\text{Ca}_2\text{-Y}$  ferrite can be attributed to the ordered to disordered transitions. Went [10] observed a minute change in slope at Curie temperature in the plot of  $\ln(\sigma)$  versus  $10^3/T$

for barium ferrite, in contrast to the marked change of slope observed in the present investigation.

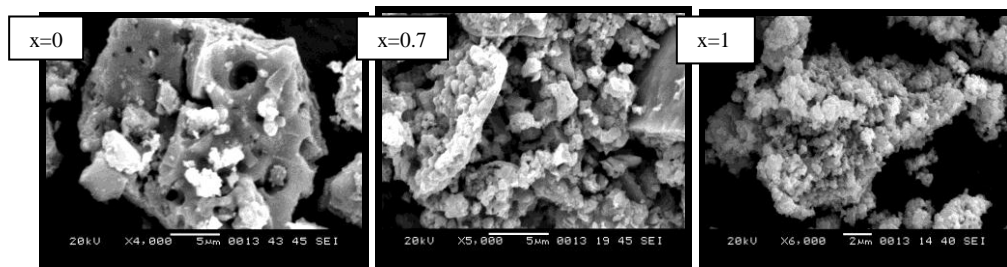


**Fig.2: SEM micrographs of  $\text{Ca}_2\text{Zn}_2\text{Fe}_{12-x}\text{Al}_x\text{O}_{22}$  : (a)  $x=0$ , (b) $x=0.7$  and (c)  $x=1$**

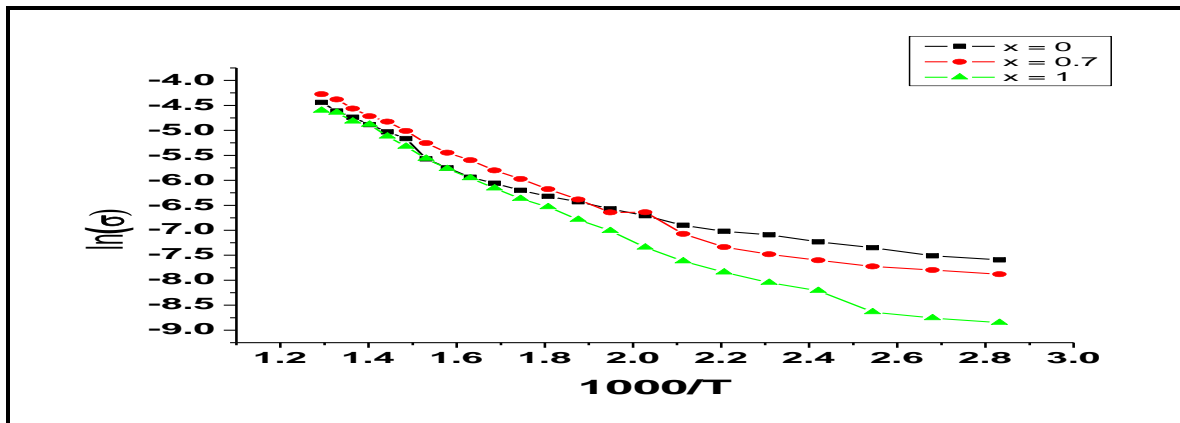


**Fig. 3: Variation of  $\ln(\sigma)$  with temperature ( $10^3/T$ ) of  $\text{Ca}_2\text{Zn}_2\text{Fe}_{12-x}\text{Al}_x\text{O}_{22}$  : (a)  $x=0$ , (b) $x=0.7$  and (c)  $x=1$**

**Table 2: Electrical resistivity ( $\rho$ ), electrical conductivity ( $\sigma$ ) at room temperature and activation energy ( $\Delta E$ ) of aluminium substituted calcium ferrite**

| Sample   | $\rho$<br>( $\Omega\text{-cm}$ ) x<br>$10^6$ | $\sigma$<br>( $\Omega^{-1}\text{cm}^{-1}$ ) x<br>$10^{-9}$ | $\Delta E$<br>(eV) |      | $T_c$<br>(K) |
|--|--|--|--------------------|------|--------------|
|  |  |  | Ferri              | Para |              |
| ( $\text{Ca}_2\text{Zn}_2\text{Fe}_{12}\text{O}_{22}$ )                  | 89.8   | 11.13  | 0.25               | 0.37 | 705          |
| ( $\text{Ca}_2\text{Zn}_2\text{Fe}_{11.3}\text{Al}_{0.7}\text{O}_{22}$ ) | 118.7  | 8.42   | 0.26               | 0.39 | 495          |
| ( $\text{Ca}_2\text{Zn}_2\text{Fe}_{11}\text{AlO}_{22}$ )                | 159.7  | 6.26   | 0.24               | 0.35 | 410          |

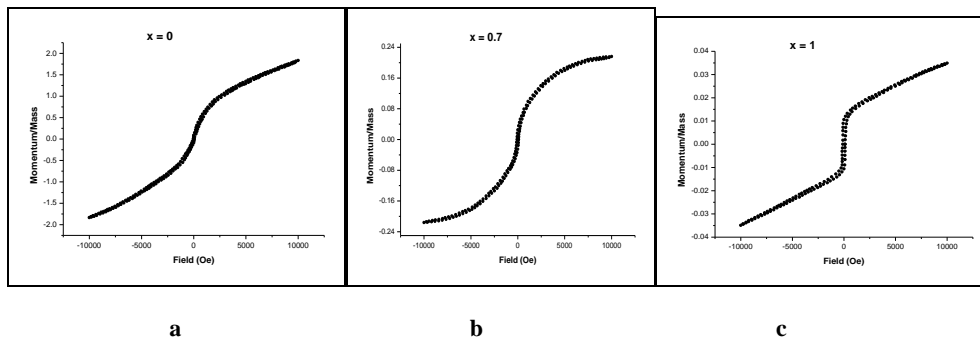


**Fig. 4:** Hysteresis loops at room temperature:  $\text{Ca}_2\text{Zn}_2\text{Fe}_{12-x}\text{Al}_x\text{O}_{22}$  : (a)  $x=0$ , (b)  $x=0.7$  and (c)  $x=1$

**Table 3:** The saturation magnetization ( $M_s$ ), remenent magnetization ( $M_r$ ), coercivity ( $H_c$ ), squareness and curie temperature ( $T_c$ ) at room temperature of samples

| Sample   | $M_s$<br>(emu/g) | $M_r$<br>(emu/g)<br>x $10^{-2}$ | $H_c$<br>(Oe) | Squareness | $T_c$<br>(K) |
|--|------------------|---------------------------------|---------------|------------|--------------|
| ( $\text{Ca}_2\text{Zn}_2\text{Fe}_{12}\text{O}_{22}$ )                  | 1.83             | 8.803                           | 37.689        | 0.0181     | 705          |
| ( $\text{Ca}_2\text{Zn}_2\text{Fe}_{11.3}\text{Al}_{0.7}\text{O}_{22}$ ) | 0.216            | 2.526                           | 89.410        | 0.1169     | 495          |
| ( $\text{Ca}_2\text{Zn}_2\text{Fe}_{11}\text{AlO}_{22}$ )                | 0.034            | 1.063                           | 105.321       | 0.3045     | 410          |

All the samples are found to be ferrimagnetic at the room temperature and remains so up to the Curie temperature ( $T_c$ ), above this temperature the compounds are paramagnetic. If non magnetic cation, such as Al are substituted for the magnetic cations, the interaction geometry changes resulting into the weakening in the super exchange interaction forces, so the decrease in saturation magnetization, retentivity, Curie temperature occurs. The presence of non-magnetic  $\text{Al}^{3+}$  ions does not change the spin direction but reduces the magnetic intensity (moment) of the sub lattice. Hence, the net magnetic moment of the compound decreases with increases in doping content of nonmagnetic materials [16].

In the present investigation, the samples have lower value of  $H_c$  (37-105Oe). The low saturation magnetization value may be explained by the fact that the particles may be monodomain. Several theories, involving surface effects, spin canting and sample inhomogeneity, have been proposed to account for the relatively low magnetization in fine particles, Shafi [17], Benito [18] on the other hand Chang [19] showed that incoherent reversal was occurring in the single domain

particles with diameter greater than 60 nm and the mode of reversal was extremely dependent on thickness of the particles.

As predicted by Stoner-Wolfarth [20] and Relph Skomski [21], the squareness (SQR) should be less than 0.5 for the single domain magnetic structure of the sample. In our case, all the sample have SQR is less (i.e. between 0.02 to 0.03) which eventually confirms the single domain structure for the samples.

## 4. CONCLUSION

Calcium hexaferrites doped with  $\text{Al}^{3+}$  ion,  $\text{Ca}_2\text{Zn}_2\text{Fe}_{12-x}\text{Al}_x\text{O}_{22}$  ( $x=0, 0.7$  and  $1.0$ ) were prepared by the microwave induced sol-gel combustion technique. The X-ray diffraction studies confirm the formation of monophase Y-type hexaferrites and the a and c values of the sample supports this

confirmation. Structural studies have confirmed the space group of the samples to be  $R\bar{3}m$  (SG no. 166). The SEM study confirmed that samples exhibit relatively well defined, hexagonal like grains with average size of less than 80 nm. The electrical conductivity of the samples increases with increase in the temperature. The conduction mechanism in calcium ferrite was explained on the basis of Verwey hopping model. The nano-range of particle size of hexaferrites helps to improve many magnetic properties mentioned earlier. The substitution of  $Al^{3+}$  ion for  $Fe^{3+}$  ion greatly improves the magnetic parameters.

## REFERENCES

- [1] Jonker G.H., Philips Tech. Rev., 18, 145 (1956).
- [2] Kojima H., Fundamental properties of hexagonal ferrites with magnetoplumbite structure, in : E.P. Wohlfarth (Ed.), Ferromagnetic Material, North-Holland Publishing Company, Amsterdam, 3, (1982).
- [3] F. Leceabue, R. Painzzieri, G. Albanese, G. Leo, N. Suarez, Mat. Res. Bull. 33 (1988) 266.
- [4] K. Haneda and H. Kojima, J. Phys. Status Solidi (A) 6 (1971) 259.
- [5] X. Wang, D. Li, X. Wang, J. Alloys. Compd. 273 (1996) 45.
- [6] D. B. Ghare, Sinha A. B. P., J. Phys. Chem. Solids, 29 ((1968) 885.
- [7] K. Haneda, H. Kojima, Jap. J. Appl. Phys, 12 (1973) 355.
- [8] S. Ounnunkad , P. Winotai , J. Magn. Magn. Mater. 301 (2006) 292.
- [9] S. Thompson, N. J. Shirtcliffe, E. S. O'Keefe, S. Appleton, C. C. Perry., J. Magn. Magn. Mater., 292 (2005) 100.
- [10] J. J.Went, G. W. Rathenau, E. W. Gorter, G. W. Oosterhout, V. Philips Tech. Rev. 13 (1952) 194.
- [11] A. Tawfik, J. Therm. analysis, 35 (1989) 141.
- [12] Sharad Sable, Ph.D. Thesis (2012).
- [13] ASM Handbook, Properties and Selection: Nonferrous Alloys and Special-Purpose Materials, ASM International, Materials Park, OH, 2 (1990).
- [14] S. Ram, H. Krishan, K.N. Rai, K.A. Narayan, Jpn. J. or App. Phy. 28 (4) (1989) 604.
- [15] O. Kalogirou , D. Samaras, H.Vincent, Solid State Ionics, 47 (1991) 31.
- [16] S. G. Lee, S. J. Kwon, J. Magn. Magn. Mater. 153 (1996) 181.
- [17] K. Shafi, Y. Koltypin , A. Gedanken , R. Prozorov , Balogh., J. Lendvai, I. Felner, J. Phys. Chem. 5B, 409(1997).
- [18] G. Benito, M. P. Morales, J. Requena, V. Raposo, M. Vazquez, J. S. Moya, JMMM 234 (2001) 645.
- [19] T. Chang, J. G. Zhu, J. H. Judy, J. Appl. Phys., 73 (1993) 6715.
- [20] E. C. Stoner, E. W. Wolfarth, Phil. Trans. Roy Soc. London, A 240 (1948) 599.
- [21] Relph Skomnski, Simple Models of Magnetism, March (2007).